Fermi National Accelerator Laboratory,
P.O. Box 500, Batavia IL, 60510

TD-05-052
12/13/2005

LARP Technology Quadrupole TQC01: 2D Magnetic Design and Analysis

V.V. Kashikhin, A.V. Zlobin

Introduction

The main goal of LARP technology quadrupole program is achieving a maximum field gradient above 200 T/m in a 90 mm aperture and demonstrating the reproducibility of main magnet parameters using 1-m long Nb_3Sn quadrupole models. The program plan includes fabrication, test and comparison of 5-6 quadrupole models based on two different mechanical structures and the same coil design. The TQC01 quadrupole design, being developed at Fermilab, is based on 2-layer shell-type coils placed inside the modified mechanical structure of LHC MQXB magnet. This note summarizes the TQC01 coil cross-section optimization and presents the results of 2D magnetic analysis.

Cable parameters

TQC01 Rutherford-type cable consists of 27 Nb_3Sn strands, 0.7-mm in diameter, produced using Modified Jelly Roll (MJR) process. The cable insulation consists of 0.125-mm thick S2-glass sleeve. The nominal cable parameters are summarized in Table 1. The cable design and the main parameters were provided by the LARP materials support group after optimizing the number of strands as well as the cable width, thickness and keystone angle.

Table 1. Cable parameters.

Parameter	Unit	Value
Number of strands	-	**27**
Strand diameter	mm	**0.700**
Bare width	mm	**10.050**
Bare inner edge thickness	mm	**1.172**
Bare outer edge thickness	mm	**1.348**
Cabling angle	deg.	**15.5**
Keystone angle	deg.	**1.000**
Radial insulation thickness	mm	**0.125**
Azimuthal insulation thickness	mm	**0.125**
Copper to non-copper ratio	-	**0.85**

2D magnetic design

The coil cross-section was optimized using ROXIE 9.0 code. The optimization goal was to achieve a maximum field gradient and the best geometrical field quality in a 90 mm aperture with a 2-layer shell-type coil using one wedge (per octant) in the inner layer and thin midplane shims (the shims are used for the field quality correction and as a midplane insulation). The optimization was performed with an additional inter-layer insulation of 0.250 mm. Magnetic properties of the collar pack were simulated by a constant magnetic permeability of 1.003 (assuming Nitronic 40 stainless steel as the collar material). Magnetic properties of the iron yoke were simulated by the B(H) curve measured on the samples of low carbon steel used in the yokes of MQXB magnets.

1st iteration

Figure 1 shows the coil quadrant cross-section with the field vectors and Figure 2 presents the position of the coil with respect to the collar and yoke with the flux distribution in the yoke at 13 kA current in the coil.

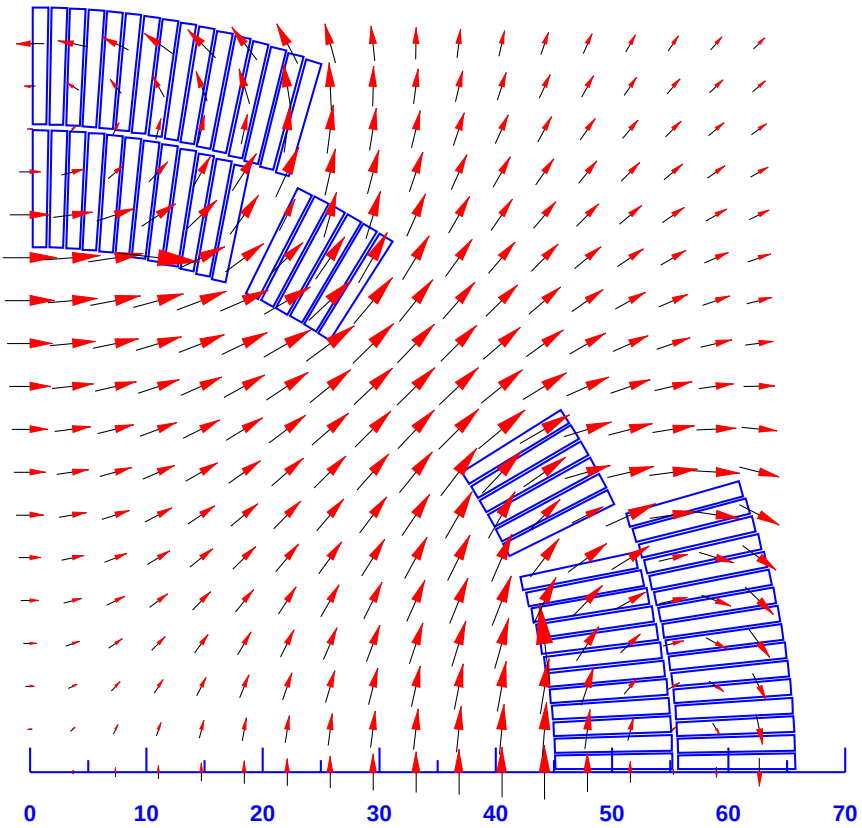

Figure 1. Coil cross-section with magnetic field vectors.

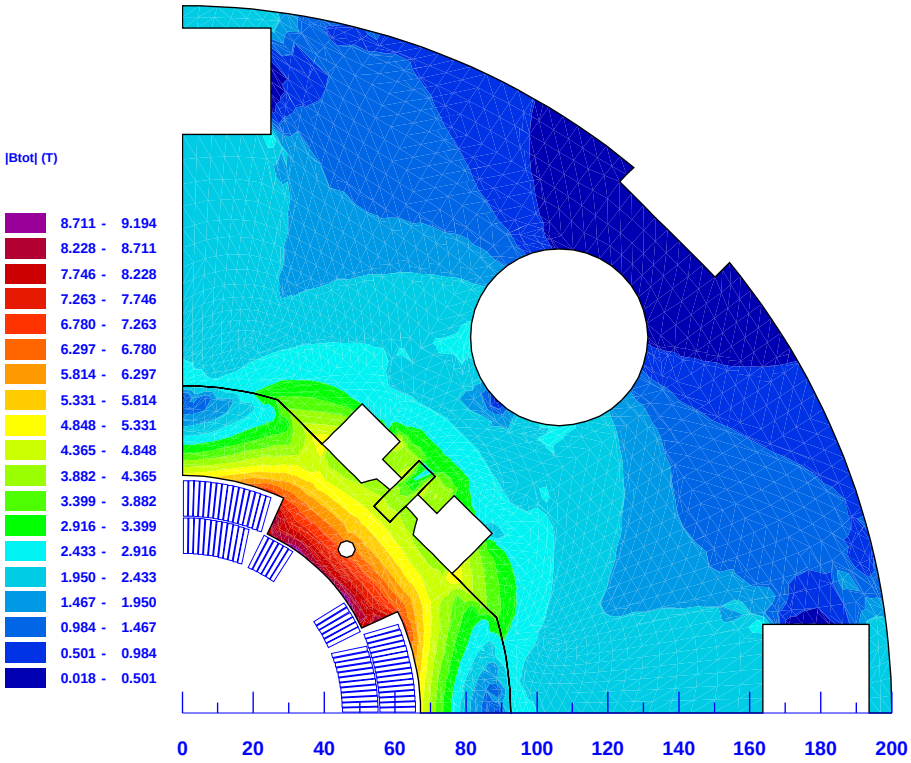

Figure 2. Yoke cross-section with the flux density diagram at 13 kA current.

The geometrical field harmonics are summarized in Table 2 and the yoke saturation effect is presented in Figure 3. The field harmonics are reasonably small at low fields. The dodecapole b_6 has a maximum at the intermediate fields due to the yoke saturation. Note that the yoke saturation effect was not specifically minimized in this magnet since the yoke structure was supposed to be borrowed unchanged from the MQXB magnet. Figure 4 shows the coil sketch with the block dimensions.

Table 2. Geometrical field harmonics at half-bore radius (I = 15 A).

n	b_n, 10^{-4}
6	0.00075
10	0.00059
14	0.01664
18	-0.00487

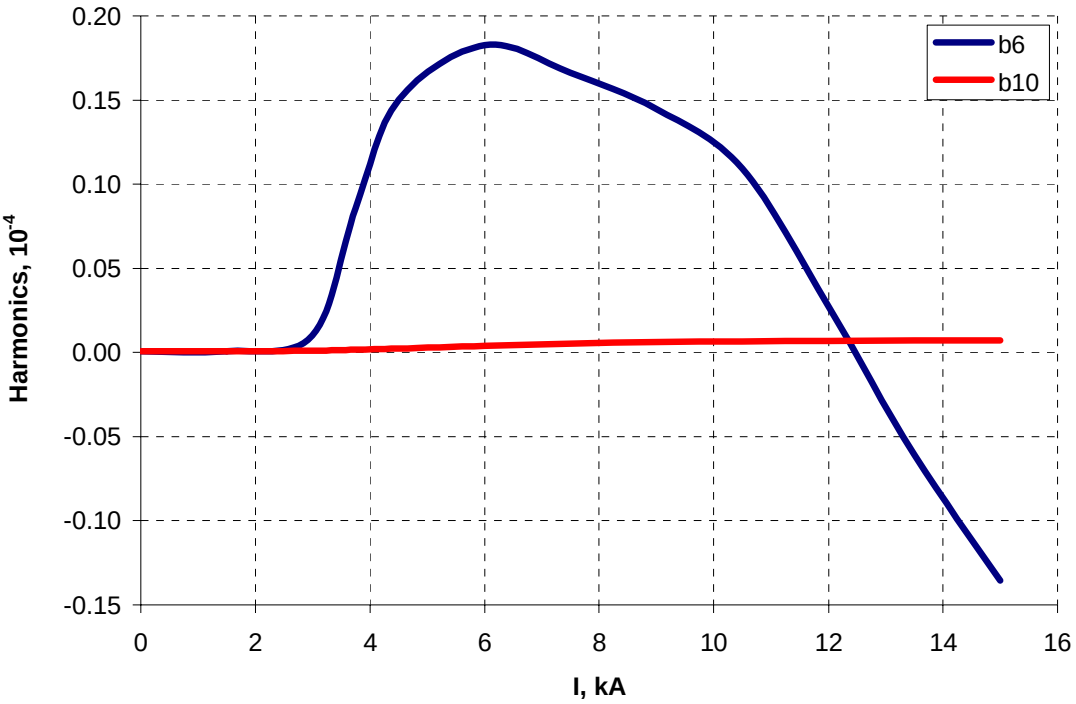

Figure 3. Harmonics variation due to iron saturation effect at half-bore radius.

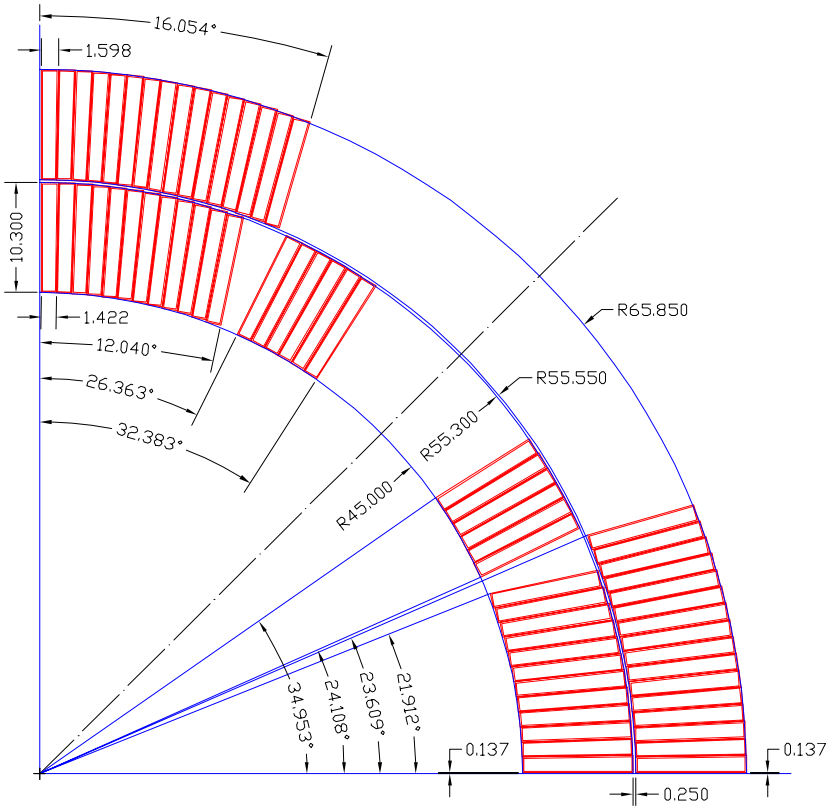

Figure 4. Coil cross-section (dimensions are in [mm]; all dimensions are for the insulated conductors).

2nd iteration

The coil cross-section, shown in Figure 4, was fixed and the parts were in procurement when the results of the mechanical analysis made it clear that the collar and yoke surfaces had to be modified to accommodate the control spacers. Figure 5 shows the magnet cross-section with the modified collar and yoke surfaces. Since the coil was optimized for the yoke design with a different inner surface, the geometrical field quality degraded and the yoke saturation effect changed as shown in Table 3 and Figure 6.

The magnet load lines are presented in Figure 7 and the quench characteristics are shown in Figures 8-9 and Table 4 at 4.2 K and 1.9 K temperatures. In the case of the MJR conductor with the critical current density of 2000 A/mm^2 at 12 T and 4.2 K the magnet quench gradient is 216 T/m at 4.2 K and 233 T/m at 1.9 K. The magnet quench currents are 13 kA and 14 kA respectively.

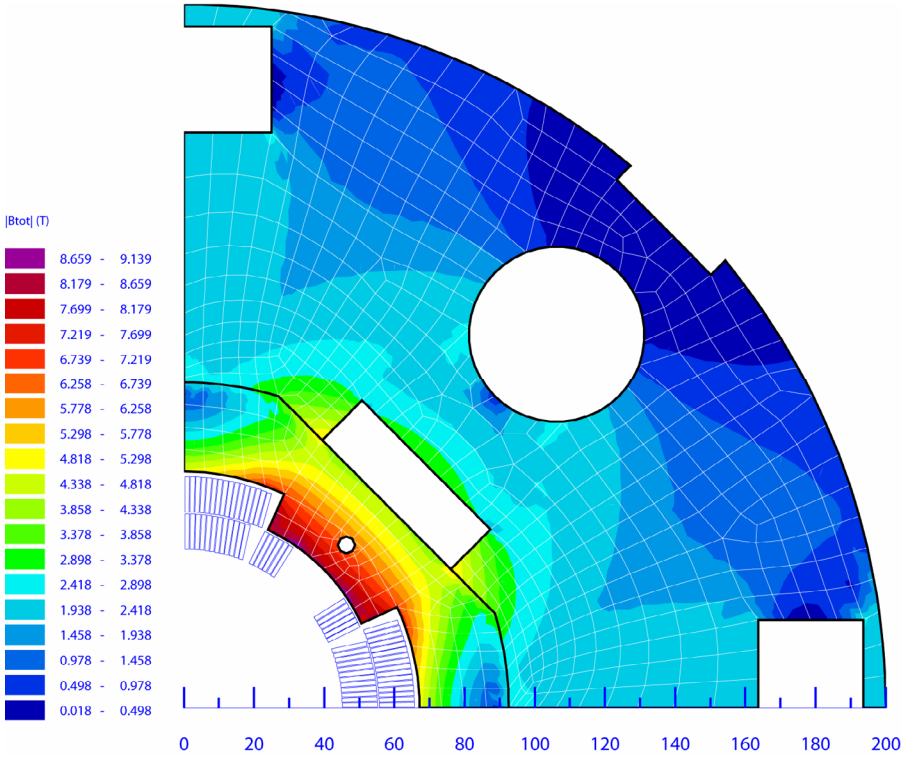

Figure 5. Yoke cross-section with the flux density diagram at 13.0 kA.

Table 3. Geometrical field harmonics at half-bore radius (I = 15 A).

n	b_n, 10^{-4}
6	0.90839
10	-0.00366
14	0.01680
18	-0.00491

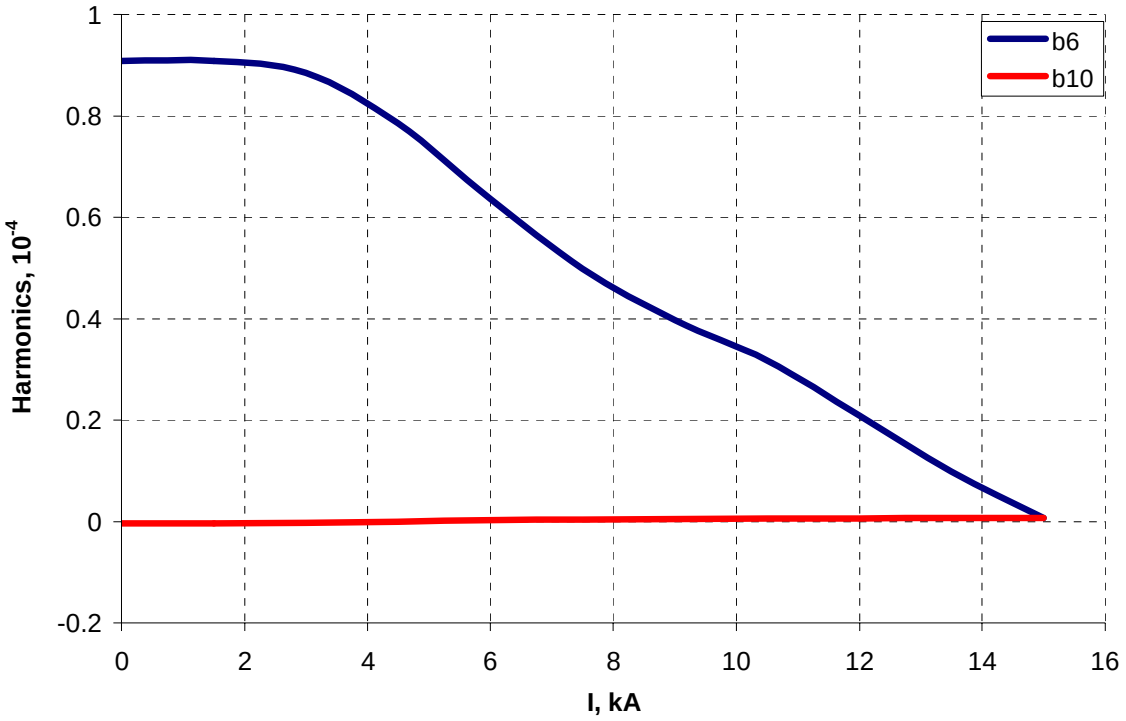

Figure 6. Harmonic variations due to iron saturation effect at half-bore radius.

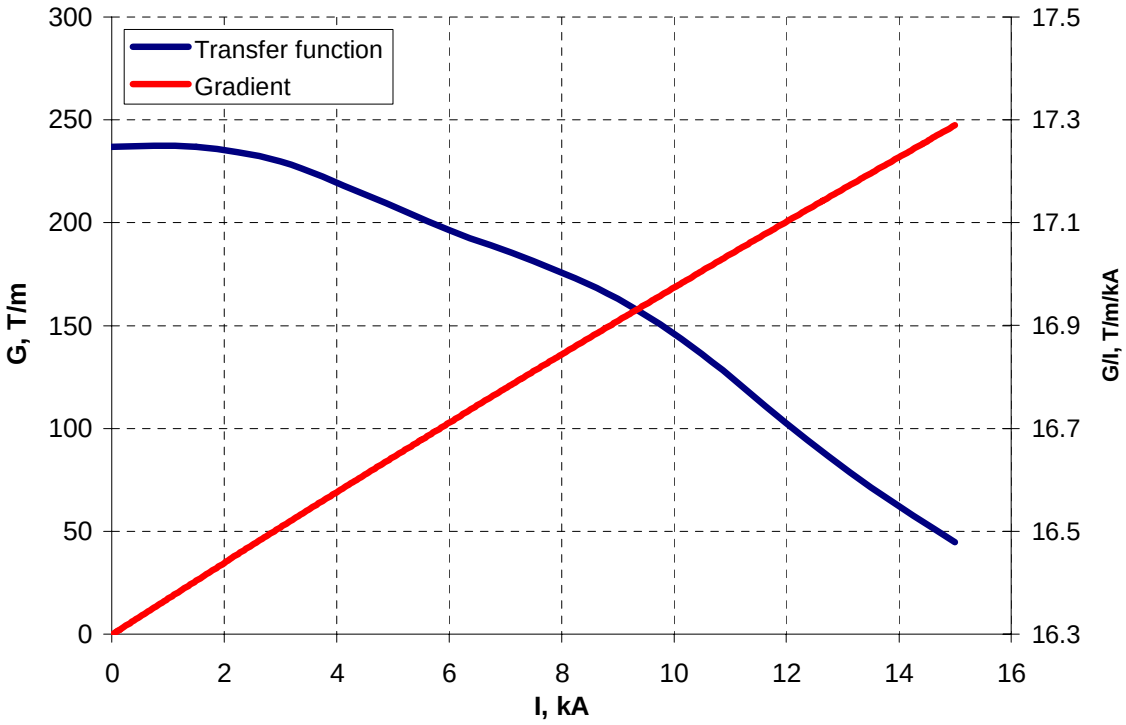

Figure 7. Transfer function and load line.

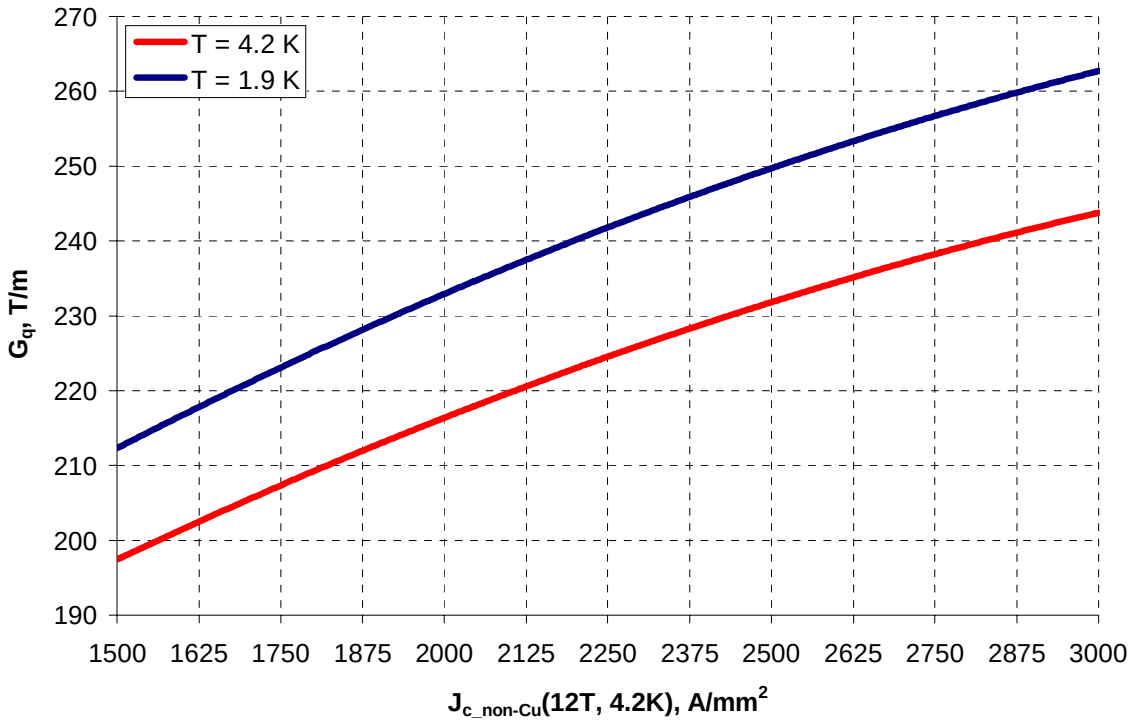

Figure 8. Quench gradient as a function of the critical current density.

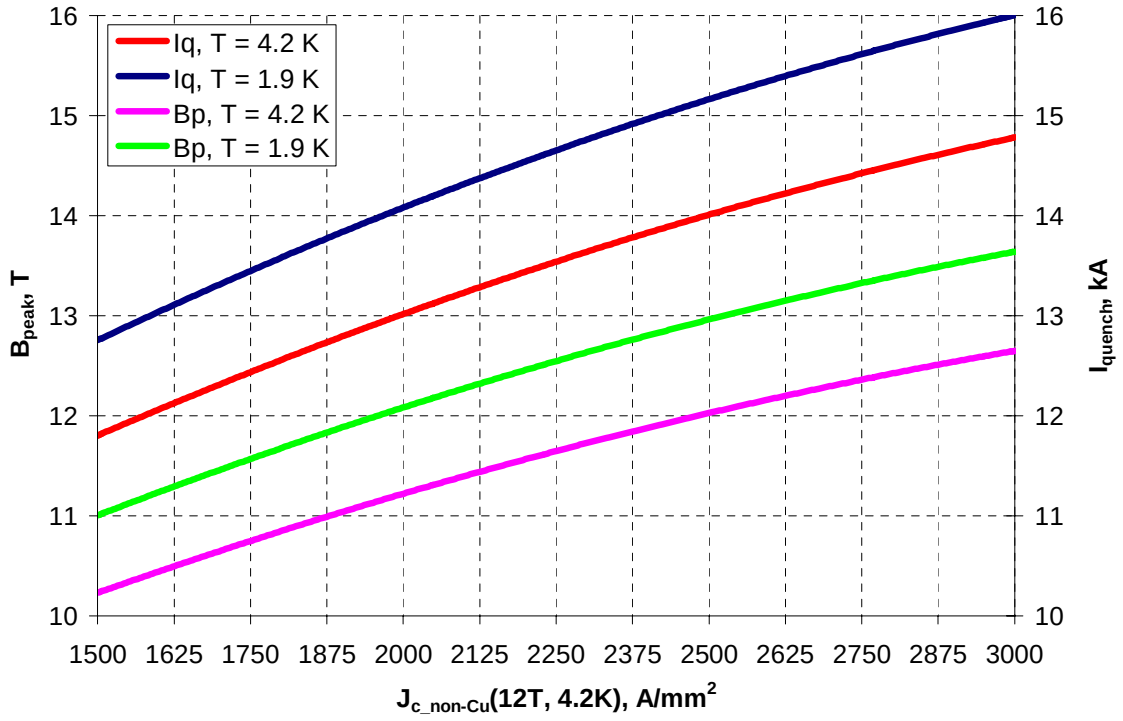

Figure 9. Quench current and peak field as functions of the critical current density.

Table 4. Magnet parameters.

Parameter		Unit	Value
N of layers		-	**2**
N of turns		-	**136**
Coil area (Cu + nonCu)		cm^2	**29.33**
Assumed non-Cu J_c at 12 T, 4.2 K		A/mm^2	**2000**
4.2 K temperature			
Quench gradient		T/m	**216.54**
Quench current		kA	**13.027**
Peak field in the coil at quench current		T	**11.233**
Magnet inductance at quench current		mH/m	**4.568**
Stored energy at quench current		kJ/m	**387.60**
Lorentz force per 1st coil octant at quench current	F_x	MN/m	**1.236**
	F_y	MN/m	**-1.828**
1.9 K temperature			
Quench gradient		T/m	**233.14**
Quench current		kA	**14.095**
Peak field in the coil at quench current		T	**12.094**
Magnet inductance at quench current		mH/m	**4.539**
Stored energy at quench current		kJ/m	**450.88**
Lorentz force per 1st coil octant at quench current	F_x	MN/m	**1.388**
	F_y	MN/m	**-2.082**